HAYATI
Journal of Biosciences

Vol. 33 No. 3, May 2026 681-693
DOI:10.4308/hjb.33.33.681-693
ISSN: 1978-3019
EISSN: 2086-4094

Research Article

Combination Effect of Culture Media and Silver Nanoparticle on the Effectiveness of Tobacco Anther Regeneration

Mohammad Nur Khozin[1*], Yusuf Dary Ahnaf[1], Parawita Dewanti[2], Didik Pudji Restanto[2], Iryono[3]

[1]*Department of Agronomy, Faculty of Agriculture, Jember University, East Java 68121, Indonesia*
[2]*Center for Development of Advanced Science and Technology (CDAST), University of Jember 68121, East Java 68121, Indonesia*
[3]*Tarutama Nusantara Agribusiness Cooperative (KOPA) Tarutama Nusantara 68121, East Java 68136, Indonesia*

ARTICLE INFO

Article history:
Received July 11, 2025
Received in revised form November 30, 2025
Accepted January 8, 2026
Available Online January 15, 2026

KEYWORDS:
anther culture,
Chu's N6,
MS,
silver nanoparticles,
tobacco

ABSTRACT

Anther culture is an effective biotechnological approach to accelerate the production of homozygous lines in tobacco breeding. This study evaluated the interaction between culture media (Murashige and Skoog/MS and Chu's N6) and silver nanoparticle (AgNP) concentrations on in vitro anther regeneration of tobacco (*Nicotiana tabacum* L.). The experiment was arranged in a completely randomized design with ten treatment combinations consisting of two basal media and five AgNP concentrations (0, 2.5, 5, 7.5, and 10 ppm), each replicated three times. Quantitative parameters included callus formation, shoot regeneration, rooting response, regeneration percentage, and contamination rate. MS medium supplemented with 2.5 ppm AgNPs (K2) produced the optimal response, showing 100% callus formation and the highest shoot regeneration percentage (89%). Root formation was observed only in treatments K2 and K4. In contrast, higher AgNP concentrations (≥7.5 ppm), particularly in Chu's N6 medium, significantly reduced regeneration percentages (ANOVA, $p<0.05$). The promotive effect of low AgNP concentration is associated with suppression of ethylene activity, antimicrobial action, and regulation of reactive oxygen species (ROS), which collectively enhance cell division and organogenesis. These findings indicate that MS medium supplemented with 2.5 ppm AgNPs is optimal for tobacco anther regeneration and suitable for doubled-haploid production.

1. Introduction

Tobacco (*Nicotiana tabacum* L.) is a seasonal crop widely cultivated in Indonesia for its high economic value. According to Statista (2024), the Gross Domestic Product (GDP) of the Tobacco Products Industry (TPI) in Indonesia in 2023 increased to 147.83 trillion rupiah, up from the previous year. However, state revenue from Tobacco excise in Indonesia in 2023 decreased by 8.33 trillion rupiah from the previous year to 210.29 trillion rupiah due to reduced national cigarette production (BPK RI 2024). Tobacco production in Indonesia has decreased by 22.6 thousand tons from 2020 to 2023 (BPS 2024). This decline is mainly attributed to a reduction in cultivated area, fluctuating climate conditions, and declining farmer interest due to unstable selling prices and higher production costs (Herawati & Yulaikah 2011). Similar trends have also been reported in other major tobacco-producing countries, where socioeconomic and climatic factors significantly influence national production levels (Rasud & Bustaman 2020). One of the efforts that can be made to increase tobacco production is by using superior varieties, such as hybrid

*Corresponding Author
E-mail Address: nurkhozin@unej.ac.id

tobacco varieties. According to Herawati & Yulaikah (2011), hybrid tobacco plants can produce 4-5 more leaves, exhibit better adaptability, uniform growth, and resistance to various diseases, including *Phytophthora nicotianae, Ralstonia solanacearum*, and Tobacco Mosaic Virus (TMV). The formation of hybrid tobacco requires pure strain plants. However, the formation of pure strains conventionally requires a process of crossing and selection repeatedly until at least the 5th offspring (F5), which requires a long time of up to 5 years more (Nurhidayah *et al.* 2023). Efforts can be made to shorten the time required of form pure strain plants, one of which is to use anther culture techniques (Tefera 2019). Plants resulting from anther culture have 100% homozygosity after being multiplied into double-haploid plants, which are achieved in one generation (Sari & Solmaz 2021). Efforts to support the regeneration of tobacco anthers include the use of nutritious culture media.

The culture medium that is often used in *in vitro* plant propagation is Murashige & Skoog (MS) because it contains more complex macro- and micronutrient formulations and vitamins. However, in some studies on rice anther culture, the nutrient medium used is Chu's N6 because it can help callus growth and differentiation (Ali *et al.* 2021). In addition, the addition of silver nanoparticles (AgNPs) supplements can help in regenerating explants by inhibiting ethylene formation, regulating Reactive Oxygen Species (ROS) (Yin *et al.* 2020). One of the major challenges in anther culture is microbial contamination, which is often inevitable even under aseptic conditions. Contamination may originate from external sources, such as air, equipment, and operator handling, or from internal sources, such as endophytic microorganisms that persist within plant tissues even after surface sterilization (Cassells 2012). To minimize contamination, several antimicrobial agents have been used in plant tissue culture media, including antibiotics such as cefotaxime, streptomycin, and kanamycin, as well as chemical sterilants like mercuric chloride and sodium hypochlorite. However, these substances can cause phytotoxic effects, including inhibition of callus proliferation, tissue necrosis, and chlorosis (Murthy *et al.* 2014; Ali *et al.* 2021). Therefore, silver nanoparticles (AgNPs) have been proposed as a more biocompatible alternative. Ag ions and reactive oxygen species (ROS) released from AgNPs can damage microbial cell membranes, proteins, and DNA, thereby reducing external and internal contamination without significantly inhibiting plant regeneration (Alfarraj *et al.* 2023; Khaldoun *et al.* 2025). Comparative studies have shown that AgNPs exhibit broader and longer-lasting antimicrobial effects than conventional antibiotics while maintaining high callus viability and promoting morphogenesis in several plant species (Ali *et al.* 2019; Alfarraj *et al.* 2023). The purpose of this study was to evaluate the effects of a combination of nutrient media treatments and the concentration of silver nanoparticles (AgNP) on the in vitro regeneration of tobacco anthers.

2.2. Materials and Methods

2.1. Explant Preparation and Sterilization

The explants were derived from stage 2 tobacco anthers, characterized by flower buds measuring 16-22 mm in length, with green petals still closed, no corolla opening, and anthers containing microspores at the uninucleate to early binucleate stage (Chuprov–Netochin *et al.* 2016). The anthers were collected from 56-63-day-old Na-Oogst tobacco plants of the H-382 variety grown in open-field conditions, as shown in Figure 1. The selected flower buds were then placed in a glass Petri dish and subjected to pre-cooling treatment at 4°C for 3 days. Low-temperature stress treatment on the anther can shift the developmental pathway from the gametophytic to sporophytic phase, which is essential for inducing microspore reprogramming into embryogenic cells, enabling haploid or doubled-haploid plant regeneration

Figure 1. Size of tobacco flower buds in stage 2

(Sood *et al.* 2021). Explant sterilization was performed under laminar airflow by immersing the flower buds in 70 % ethanol for 30-60 s, followed by 1 % sodium hypochlorite (NaClO) for 15 min, and rinsing twice with sterile distilled water for 3 min each. The treatment combinations and their respective codes are presented in Table 1.

2.2. Culture Environment and Data Analysis

The media used were basal media (MS and Chu's N6) with varying nutrient concentrations, as shown in Table 2. The two basal media were each given 30 g/L sucrose, 0.5 ppm NAA, 1 ppm BAP (El-Fiki *et al.* 2015), and AgNPs according to the treatment (0, 2.5, 5, 7.5, and 10 ppm) (Ewais *et al.* 2015) - which was then homogenized, and the pH, in the range of 5.8-6.2, was adjusted to 8 g/L agar, and the mixture was autoclaved for 30 minutes at 121°C under 15 psi.

Each treatment was repeated 3 times, yielding 30 experimental units. Each experimental unit consisted of a single 90 mm Petri dish containing 9 anthers. The planted explants were then incubated at 26°C under white fluorescent tube lamps with a photoperiod of 16 hours of light and 8 hours of darkness, with light intensity of approximately 2000 lux, positioned about 40 cm above the Petri dishes. Quantitative data on the early stages of explant development, including swelling, callus formation, bud initiation, and rooting, were recorded when explants exhibited visible signs of each stage. The regeneration process in tobacco anther culture consisted of five main stages: (1) induction, characterized by swelling of the anther tissue as an early response to stress and hormonal stimulation; (2) initiation, indicated by the formation of friable or compact callus on the surface of the anther; (3) germination, marked by the appearance of green spots or meristematic nodules on the callus surface; (4) maturation, observed as the differentiation of shoots or plantlets with developed leaves and stems; and (5) rooting, identified by root emergence from the basal part of regenerated shoots. The quantitative parameters measured at each stage included the time to initial appearance (days), the percentage of responding explants (%), and the number of organs formed (buds or roots). These parameters were used to evaluate the efficiency of each treatment in supporting the sequential stages of anther regeneration. Meanwhile, data on the

Table 1. Treatment codes of the combination of nutrient media+AgNPs supplement concentration

Treatment code	Nutrient media + AgNPs supplement concentration
K1	MS+0 ppm AgNPs
K2	MS+2.5 ppm AgNPs
K3	MS+5 ppm AgNPs
K4	MS+7.5 ppm AgNPs
K5	MS+10 ppm AgNPs
K6	Chu's N6+0 ppm AgNPs
K7	Chu's N6+2.5 ppm AgNPs
K8	Chu's N6+5 ppm AgNPs
K9	Chu's N6+7.5 ppm AgNPs
K10	Chu's N6+10 ppm AgNPs

Note: All treatments were supplemented with 0.5 ppm NAA and 1 ppm BAP in addition to the combinations listed above. K1 = MS + 0 ppm AgNPs; K2 = MS + 2.5 ppm AgNPs; K3 = MS + 5 ppm AgNPs; K4 = MS + 7.5 ppm AgNPs; K5 = MS + 10 ppm AgNPs; K6 = Chu's N6 + 0 ppm AgNPs; K7 = Chu's N6 + 2.5 ppm AgNPs; K8 = Chu's N6 + 5 ppm AgNPs; K9 = Chu's N6 + 7.5 ppm AgNPs; K10 = Chu's N6 + 10 ppm AgNPs

Table 2. Composition of MS and Chu's N6 media in 1 liter

Nutrients	MS	Chu's N6
Macro		
NH_4NO_3	1.650 g	-
$(NH_4)_2SO_4$	-	463 mg
KNO_3	1.900 g	2.830 g
$CaCl_2.2H_2O$	440 mg	125.33 mg
$MgSO_4.7H_2O$	370 mg	90.37 mg
KH_2PO_4	170 mg	400 mg
Micro		
$MnSO_4.4H_2O$	22.3 mg	3.3 mg
$ZnSO_4.7H_2O$	8.6 mg	1.5 mg
H_3BO_3	6.2 mg	1.6 mg
KI	0.83 mg	0.8 mg
$FeSO_4.7H_2O$	27.8 mg	27.85 mg
$Na_2.EDTA.2H_2O$	37.3 mg	37.25 mg
$CoCl_2.6H_2O$	0.025 mg	-
$CuSO_4.5H_2O$	0.025 mg	-
$Na_2MoO_4.2H_2O$	0.25 mg	-
Vitamins		
Glycine	2 mg	2 mg
Nicotinic Acid	5 mg	0.5 mg
Pyridoxine.HCl	0.5 mg	0.5 mg
Thiamine.HCl	0.5 mg	1 mg
Myo-inositol	100 mg	-
Folic Acid	0.5 mg	-
Biotin	0.05 mg	-

parameters of the percentage of explants swelling, callus, budding, and rooting, as well as the percentage of media contaminated with fungi and bacteria, were monitored and recorded every day from the start of culture until 150 days after incubation.

2.3. Data Collection and Observation Parameters

Quantitative data were collected at each stage of explant development, including induction, initiation, germination, maturation, and rooting. The parameters observed were:

Induction stage: time (days) and percentage of anthers showing swelling response.

Initiation stage: time and percentage of callus formation, and callus growth rate.

Maturation stage: number of shoots and leaf formation.

Rooting stage: number of roots and percentage of rooted explants.

Quantitative observations were recorded every 3 days up to 150 days of culture.

2.4. Qualitative Observation

Qualitative parameters included callus color, texture, and surface morphology. Callus color was evaluated against the Munsell Color Chart, and callus texture was assessed by gentle handling with sterile forceps in the laminar airflow cabinet. Qualitative observations were made concurrently with quantitative measurements to provide complementary descriptive data.

2.5. Scanning Electron Microscopy (SEM) Analysis

SEM analysis was conducted at the end of the culture period to examine the micro-morphological characteristics of regenerated tissues. SEM observations were performed to confirm the surface structure of callus and bud development and to detect morphological changes in callus and bud development caused by AgNP exposure that could not be observed under a light microscope (Yan & Chen 2019).

2.6. Statistical Analysis

Quantitative data were statistically analyzed using Analysis of Variance (ANOVA) to determine significant differences among treatments. If significant differences were found, data were further analyzed using Duncan's Multiple Range Test (DMRT) at a 95% confidence level.

3. Results

3.1. Initial Appearance of Explant Swelling, Callus Formation, Bud Emergence, and Root Initiation

The fastest swelling, callusing, and budding explants were shown in treatment K2 (MS + 2.5 ppm AgNPs). The longest swelling and callus explants were shown in treatments K9 (Chu's N6 + 7.5 ppm AgNPs) and K10 (Chu's N6 + 10 ppm AgNPs). The longest explant-budding time was observed in treatment K6 (Chu's N6 + 0 ppm AgNPs). The fastest root emergence was in treatment K4 (MS + 7.5 ppm AgNPs). The initial appearance of explant swelling, callus formation, bud emergence, and root initiation across treatments is shown in Figure 2.

3.2. Percentage of Swelling, Callus, Budded, and Rooted Explants

Data on the percentage of swelling, callus, bud, and root explants are shown in Table 3. In all treatments, the percentage of explant swelling was 100%. The highest percentage of calloused explants was observed in treatments K1 (MS + 0 ppm AgNPs) and K2 (MS + 2.5 ppm AgNPs), of 100%. The lowest percentage of callus explants was observed in treatment K10 (Chu's N6 + 10 ppm AgNPs), at only 33%. The highest percentage of budded explants was observed in treatment K2 (MS + 2.5 ppm AgNPs), while the lowest was in treatments K9 (Chu's N6 + 7.5 ppm AgNPs) and K10 (Chu's N6 + 10 ppm AgNPs), which could not grow shoots at all. The highest percentage of budded explants was observed in treatments K2 (MS + 2.5 ppm AgNPs) and K4 (MS + 7.5 ppm AgNPs), whereas the other treatments failed to grow roots.

3.3. Number of Buds and Roots

Data on the number of buds and roots are shown in Figure 3, which shows that the highest number of buds was in K1 (MS + 0 ppm AgNPs). Buds were formed only in treatments K2 (MS + 2.5 ppm AgNPs) and K4 (MS + 7.5 ppm AgNPs), with the same number in each treatment. Visualization of bud data is shown in Figure 4, and roots in Figure 5.

3.4. Percentage of Media Contaminated with Fungus or Bacteria

Data on the percentage of contaminated media are shown in Figure 6, which indicates that all treatment media

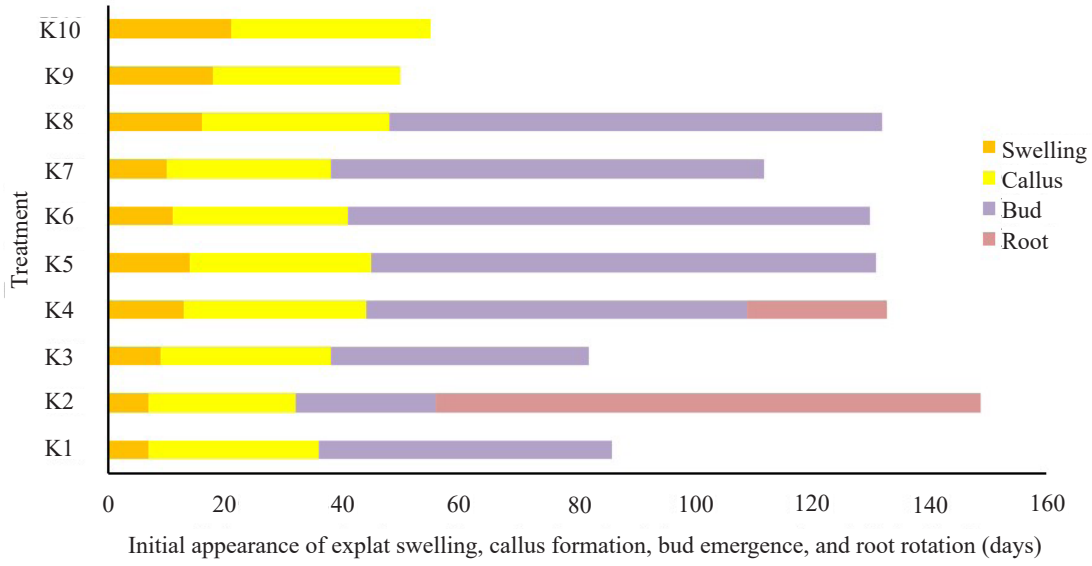

Figure 2. Initial appearance of explant swelling, callus formation, bud emergence, and root initiation. K1: MS + 0 ppm AgNPs, K2: MS + 2.5 ppm AgNPs, K3: MS + 5 ppm AgNPs, K4: MS + 7.5 ppm AgNPs, K5: MS + 10 ppm AgNPs, K6: Chu's N6 + 0 ppm AgNPs, K7: Chu's N6 + 2.5 ppm, AgNPs, K8: Chu's N6 + 5 ppm AgNPs, K9: Chu's N6 + 7.5 ppm AgNPs, K10: Chu's N6 + 10 ppm AgNPs

Table 3. Percentage of swelling, callus, bud, and root explants

Treatment code	Percentage of explants (%)			
	Swelling	Callus	Buds	Roots
K1	100	100^{a}	44^{b}	0
K2	100	100^{a}	89^{a}	11
K3	100	89^{a}	44^{b}	0
K4	100	78^{a}	33^{b}	11
K5	100	78^{a}	11^{b}	0
K6	100	100^{a}	22^{b}	0
K7	100	78^{a}	33^{b}	0
K8	100	67^{ab}	11^{b}	0
K9	100	44^{bc}	0^{b}	0
K10	100	33^{c}	0^{b}	0

Note: K1 = MS + 0 ppm AgNPs; K2 = MS + 2.5 ppm AgNPs; K3 = MS + 5 ppm AgNPs; K4 = MS + 7.5 ppm AgNPs; K5 = MS + 10 ppm AgNPs; K6 = Chu's N6 + 0 ppm AgNPs; K7 = Chu's N6 + 2.5 ppm AgNPs; K8 = Chu's N6 + 5 ppm AgNPs; K9 = Chu's N6 + 7.5 ppm AgNPs; K10 = Chu's N6 + 10 ppm AgNPs. Different letters within the same column indicate significant differences according to DMRT ($p<0.05$)

are contaminated with either fungi or bacteria. Treatments with the highest percentage of contaminants in treatment K1 (MS + 0 ppm AgNPs) and K6 (Chu's N6 + 0 ppm AgNPs). Treatments K2 - K5 and K7 - K10 showed a slightly lower percentage of contaminants. Visualization of the data on the percentage of contaminants and the level of spread of contaminants on the culture media can be seen in Figure 7. In the K1 (MS + 0 ppm AgNPs) and K6 (Chu's N6 + 0 ppm AgNPs) treatments, the level of spread of contaminants is wide enough to almost cover the entire media in the petri dish. While the K2-K5 and K7-K10 treatments showed a less diffuse level of spread.

3.5. Callus Colour and Texture

Determination of callus color is done by matching it to the color found in the Munsell color chart. The results of callus color in each treatment showed that almost all had a green-yellow color, except for the color of callus in treatment K6 (Chu's N6 + 0 ppm AgNPs) and K10 (Chu's N6 + 10 ppm AgNPs), which had a yellow color. Determination of callus texture was done by holding the callus using sterile tweezers in the LAF. The results of callus texture showed that almost all treatments had a compact texture, except for treatments K4 (MS + 7.5 ppm AgNPs) and K5 (MS + 10 ppm AgNPs), which had an intermediate texture. Data on the color and texture of the callus are shown in Table 4.

3.6. SEM Analysis

SEM (Scanning Electron Microscopy) analysis aims to observe the surface structure of explants that have exhibited growth and development responses as a result of the treatment. The sample used came from treatment K4 (MS + 7.5 ppm AgNPs).

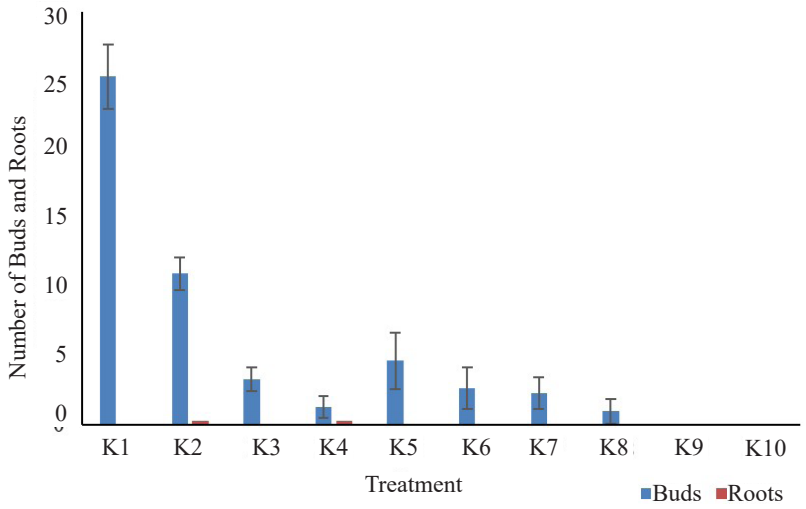

Figure 3. Number of buds and roots. K1: MS + 0 ppm AgNPs, K2: MS + 2.5 ppm AgNPs, K3: MS + 5 ppm AgNPs, K4: MS + 7.5 ppm AgNPs, K5: MS + 10 ppm AgNPs, K6: Chu's N6 + 0 ppm AgNPs, K7: Chu's N6 + 2.5 ppm AgNPs, K8: Chu's N6 + 5 ppm AgNPs, K9: Chu's N6 + 7.5 ppm AgNPs, K10: Chu's N6 + 10 ppm AgNPs

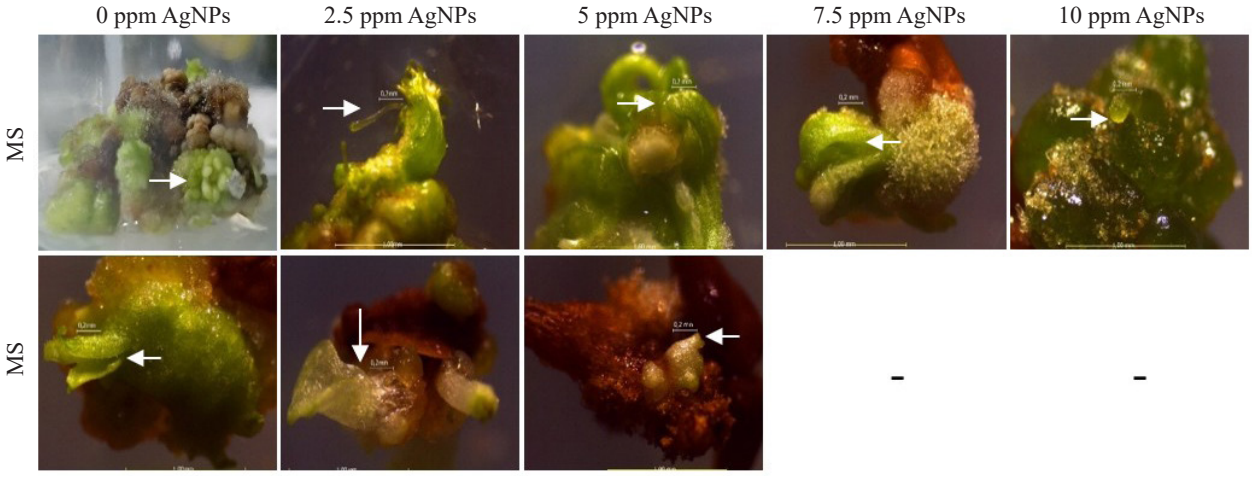

Figure 4. Visualization of the number of buds in each treatment with a magnification of 16x (white arrow) at 80 days after culture

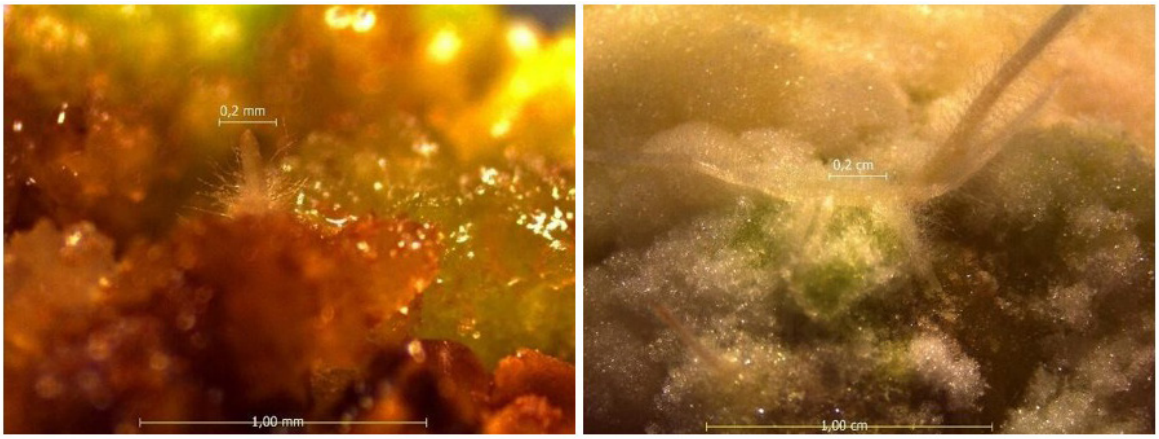

Figure 5. Visualization of the number of roots with a magnification of 16x (white arrow). K2: MS + 2.5 ppm AgNPs (right) and K4: MS + 7.5 ppm AgNPs (left) at 120 days after culture

4. Discussion

4.1. Effect of Media Composition and Nutrients

Tobacco anthers grown in MS medium showed a better regeneration response than Chu N6 medium, with the K2 treatment (MS + 2.5 ppm AgNP) being the best. This is related to the nutrient composition of both media. MS medium contains higher concentrations of the macronutrients N, Ca, and Mg than N6 (which is rich in P, K, and S), and is more complete in micronutrients (Mn, Zn, B, Co, Cu, and Mo). Nitrogen is vital because it is a major component of chlorophyll, amino acids, proteins, and nucleic acids that support plant tissue formation (Wang *et al.* 2024). Calcium in MS is essential for cell wall integrity; Ca forms calcium-pectate bridges in the middle lamella, which stabilize the wall structure, act as enzyme cofactors, and facilitate the uptake of other nutrients (Wdowiak *et al.* 2024). Magnesium also acts as a cofactor for many enzymes (e.g., in photosynthesis) and regulates the uptake of phosphate and potassium (Harris *et al.* 2018). Therefore, although N6 is rich in P, K, and S,

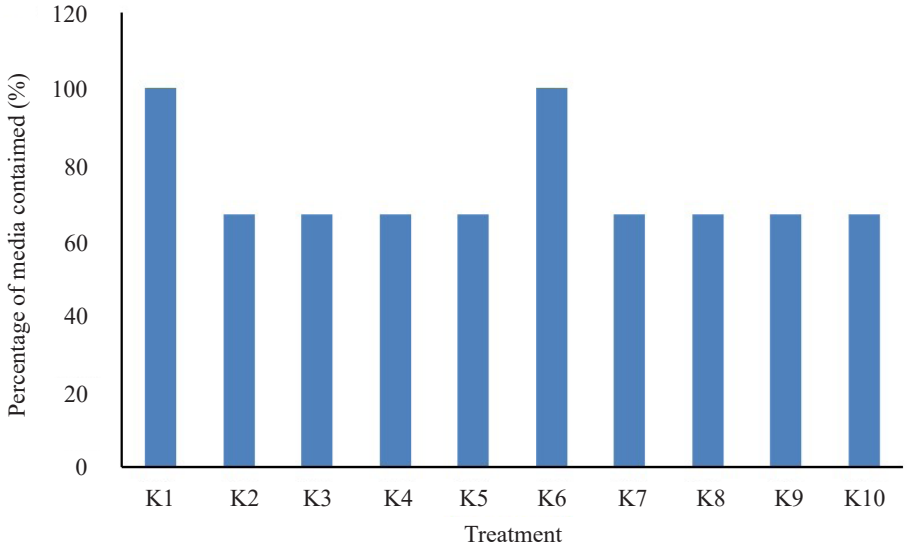

Figure 6. Percentage of media contaminated with fungi or bacteria. K1: MS + 0 ppm AgNPs, K2: MS + 2.5 ppm AgNPs, K3: MS + 5 ppm AgNPs, K4: MS + 7.5 ppm AgNPs, K5: MS + 10 ppm AgNPs, K6: Chu's N6 + 0 ppm AgNPs, K7: Chu's N6 + 2.5 ppm AgNPs, K8: Chu's N6 + 5 ppm AgNPs, K9: Chu's N6 + 7.5 ppm AgNPs, K10: Chu's N6 + 10 ppm AgNPs

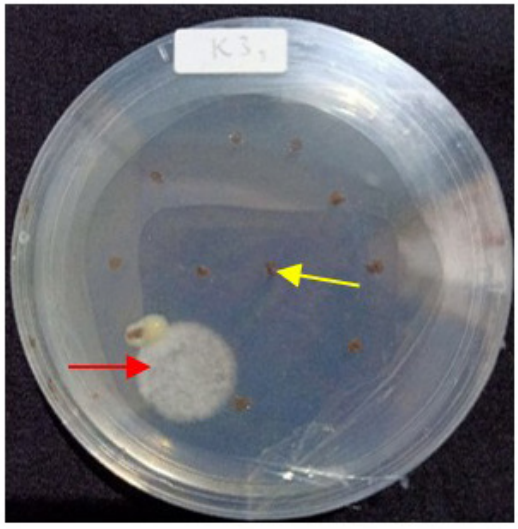

Figure 7. Visualization of a contaminant. Contaminant (red arrow), Tobacco anther explant (yellow arrow)

Table 4. Color and texture of callus in each treatment

Treatment code	Color	Texture
K1	Green-yellow	Compact
K2	Green-yellow	Compact
K3	Green-yellow	Compact
K4	Green-yellow	Intermediates
K5	Green-yellow	Intermediate
K6	Yellow	Compact
K7	Green-yellow	Compact
K8	Green-yellow	Compact
K9	Green-yellow	Compact
K10	Yellow	Compact

Note: K1 = MS + 0 ppm AgNPs; K2 = MS + 2.5 ppm AgNPs; K3 = MS + 5 ppm AgNPs; K4 = MS + 7.5 ppm AgNPs; K5 = MS + 10 ppm AgNPs; K6 = Chu's N6 + 0 ppm AgNPs; K7 = Chu's N6 + 2.5 ppm AgNPs; K8 = Chu's N6 + 5 ppm AgNPs; K9 = Chu's N6 + 7.5 ppm AgNPs; K10 = Chu's N6 + 10 ppm AgNPs

its utilization efficiency is reduced without sufficient Ca and Mg support. In addition, MS provides essential micronutrients: for example, manganese (Mn) is required for the PSII oxygen-evolving complex (water-splitting reaction) (Alejandro *et al.* 2020); Zinc (Zn) acts as an enzymatic cofactor (such as carboxylic anhydrase and SOD) and plays a role in auxin regulation and root growth (Kimura *et al.* 2023); Boron (B) facilitates nitrogen and auxin metabolism for root cell division (Brdar-Jokanović 2020); Cobalt (Co) is required in vitamin B12 for nitrogen-fixing enzymes (Hu *et al*. 2021); Copper (Cu) is a cofactor in photosynthesis, respiration, and the antioxidant system (Xu *et al.* 2024); and molybdenum (Mo) is involved in hormone synthesis, nitrogen assimilation, and purine metabolism (Rana *et al.* 2020).

Vitamins and organic compounds also have important effects. MS medium contains biotin, folic acid (B9), and myo-inositol, which are not present in N6. Biotin is a cofactor for carboxylase enzymes in primary metabolism (helping to form lipid membranes and provide energy for root cells) (Che *et al.* 2003). Folic acid is a precursor of tetrahydrofolate for one-carbon transfer reactions essential for the synthesis of purines, pyrimidines, and amino acids (Ayala-Rodríguez *et al.* 2017). Myo-inositol is required for the synthesis of membrane phospholipids and cell wall polysaccharides (pectin) and is known to facilitate the uptake of micronutrient metal ions (e.g., Zn) (Hu *et al*. 2020; Amaral & Brown 2022). Thus, MS media, richer in nutrients, micronutrients, and vitamins, promote accelerated explant growth and development (callus, shoot, and root formation). It is also noteworthy that explant preparation (cutting and sterilization) causes tissue injury, triggering Ca^{2+} uptake and a surge in ROS to initiate the healing process and callus formation. The complete nutritional content of MS supports these biochemical processes.

4.2. Influence of Culture Conditions on Regeneration Stages

The data showed that the K2 treatment (MS + 2.5 ppm AgNP) resulted in the fastest anther swelling, callus formation, and shoot emergence, while the Chu N6 treatment with high AgNP (K9, K10) was the slowest. This difference is primarily due to media composition and hormone interactions. The initial induction phase (swelling) is driven by the hormone auxin, which activates the expansin and XTH genes, loosening cell walls, allowing water to enter, and increasing turgor pressure (Cosgrove 2022). Wounding caused by explant preparation also triggers an influx of Ca^{2+} and a surge of ROS, activating a series of healing signals that trigger callus formation (Minibayeva *et al.* 2015; Ikeuchi *et al.* 2019). Afterward, the rate of callus formation is largely influenced by endogenous explant hormones and cytokinins in the media. The addition of cytokinin (BAP) stimulates cell division, resulting in compact callus formation (rapid cell wall lignification) (Rasud & Bustaman 2020; Ningrum 2024).

During the organogenesis phase, the number of shoots and roots is strongly influenced by the auxin:cytokinin ratio. Treatment without AgNP (K1) produced the highest number of shoots due to high auxin accumulation (AgNP actually reduces auxin receptor expression, shifting the auxin:cytokinin ratio to a lower level) (Sun *et al.* 2017). Conversely, treatments with moderate levels of AgNP (K2, K3) resulted in faster root emergence; this occurs because although AgNP suppresses auxin accumulation, endogenous auxin levels in these treatments remain high enough to stimulate root formation (Stoynova-Bakalova *et al.* 2022). In general, nanoparticles such as AgNP are known to regulate hormonal pathways and oxidative stress, thereby enhancing organogenesis (including callus formation, shoot division, and rooting). In other words, culture conditions (media type, AgNP concentration, hormone administration) synergistically affect the rate of swelling, callus formation, shoot and root formation in accordance with plant physiological mechanisms.

4.3. Quantitative Response of Explants

Quantitative data on the developmental response of tobacco anther explants at each stage of regeneration showed clear differences among the treatments. The induction stage, indicated by explant swelling, occurred in all treatments with a 100% response rate; however, the fastest response time was recorded in K2 (MS + 2.5 ppm AgNPs), followed by K1 (MS + 0 ppm AgNPs), while the slowest was in K9 (Chu's N6 + 7.5 ppm AgNPs) and K10 (Chu's N6 + 10 ppm AgNPs).

At the initiation stage, the highest percentage of callus formation (100%) was also observed in K1 and K2, whereas the lowest (33%) occurred in K10. The average time to callus appearance was significantly shorter in MS-based media than in Chu's N6-based media, indicating the stronger nutritional support of MS for early cell proliferation.

During the maturation stage, which was characterized by bud emergence, the largest number of buds was recorded in K1 (MS + 0 ppm AgNPs), followed by K2

(MS + 2.5 ppm AgNPs) and K4 (MS + 7.5 ppm AgNPs). In contrast, the Chu's N6 treatments with higher AgNP concentrations (K9 and K10) failed to produce buds.

At the rooting stage, root formation occurred only in K2 and K4, both of which showed the same average number of roots per explant, whereas other treatments exhibited no rooting response. Statistical analysis (ANOVA, $p<0.05$) confirmed significant differences among treatments for all measured quantitative parameters—time of appearance, percentage of responding explants, and number of organs formed. Duncan's Multiple Range Test (DMRT) further identified K2 (MS + 2.5 ppm AgNPs) as the most effective combination for supporting the sequential stages of tobacco anther regeneration.

4.4. Qualitative Characteristics of Callus

The results of callus color in Table 4 also show that most treatments produce green-yellow callus color caused by nutrients in more complex media and the provision of AgNPs in the culture media. According to Azadi *et al.* (2021), the provision of AgNPs in culture media can increase the uptake of N, Mg, and Fe, which are involved in chlorophyll biosynthesis. In line with the results of research by Satya *et al.* (2024), the addition of AgNPs to the culture medium can increase the amount of chlorophyll a and b in *Maerua oblongifolia* plants. This can occur because AgNPs inhibit ethylene formation and activity, leading to chlorophyll degradation (Azadi *et al.* 2021). Callus color data (Table 4) for the K6 and K10 treatments are yellow. It is suspected that tobacco anther explants experience nutritional stress because the nutrient content in Chu's N6 media is not complex and tends to have a low concentration. So that if the tobacco anther is planted on Chu's N6 media supplemented with high concentrations of AgNPs, the oxidative stress caused by the AgNPs may overwhelm the nutrients in the media, which cannot counteract the stress. According to Iori *et al.* (2023), high concentrations of AgNPs can cause excessive ROS production, resulting in a yellow callus color.

The formation of callus texture can be influenced by the synergistic effect of endogenous auxin and cytokinin hormones given to the explants. The callus texture shown in Table 4 indicates that all calli are compact, with only K4 and K5 exhibiting an intermediate texture. The intermediate callus texture comes from a combination of compact and friable callus textures. According to Ningrum (2024), cytokinin addition to the media can increase cell division, making the callus more compact as cell walls form more quickly and undergo lignification. In addition, the compact callus texture is also caused by differences in the ability of plant tissues to absorb nutrients, especially N and growth regulators in the culture media (Silvina *et al.* 2022). Callus with a compact texture is good callus for organogenesis, while crumbly callus is used in callus induction to produce secondary metabolites. Friable callus can occur because its cells undergo rapid division. According to Silvina *et al.* (2022), a callus with a crumbly texture can increase oxygen diffusion between cells, making it suitable for suspension culture because it contains single cells that are easy to separate.

4.5. SEM Analysis and Morphological Changes

SEM analysis revealed distinct changes in the microstructure of the tissue surface due to AgNP treatment. In sample K4 (MS + 7.5 ppm AgNPs), compact callus structures with emerging bud primordia were observed before SEM analysis, while SEM images showed elongated epidermal-like cells and numerous microscopic pores on the callus and shoot surfaces (Figure 8). These irregularities indicate altered cell wall integrity and differentiation processes under AgNP exposure. This finding is consistent with previous studies reporting that AgNPs can penetrate cell walls and trigger the formation of new pores, leading to membrane disruption and cytoplasmic shrinkage. AgNPs accumulated in plasmodesmata (50-60 nm in size) may inhibit intercellular communication and nutrient transport. Thus, SEM observations confirm that AgNP treatment modifies the microstructure of explant surfaces by forming pores and altering tissue organization, aligning with the known antimicrobial and cytotoxic effects of AgNPs (Yan & Chen 2019; More *et al.* 2023).

4.6. Anticontaminant Effect and Statistical Interpretation

AgNPs also act as anticontaminant agents. Ag^+ ions and ROS from AgNPs are known to damage microbial membranes, proteins, and DNA, thereby reducing contamination without significantly inhibiting plant regeneration. Compared to traditional antibiotics, AgNPs provide a broader and longer-lasting antimicrobial effect. In this study, although contamination levels in media with AgNPs (especially K2) were reduced, none of the treatments were completely free of contaminants. Alfarraj *et al.* (2023) showed that the inhibitory effect of AgNP on bacterial/fungal growth was significant only at concentrations >20 ppm. In contrast, concentrations of 0-10 ppm (as in this experiment) were insufficient for

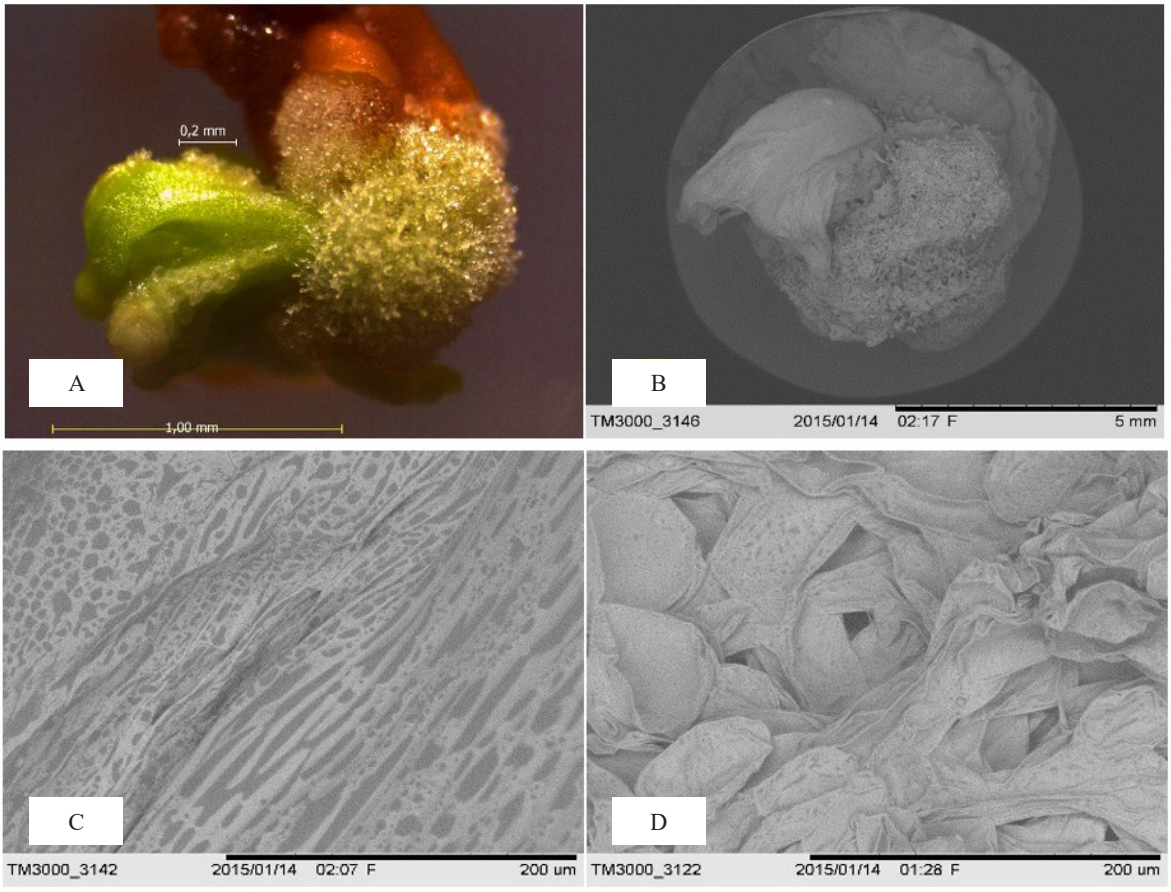

Figure 8. Visualization of callus condition in treatment K4: MS + 7.5 ppm AgNPs before and after SEM analysis. (A) Callus surface before SEM showing compact callus with emerging bud primordia. (B) SEM overview of callus–bud complex morphology at 5 mm magnification. (C) SEM image showing elongated epidermal-like cells indicating early differentiation (200 mm magnification). (D) SEM image showing pore-like openings and irregular cell surfaces caused by AgNP treatment (200 mm magnification). Arrows in each image indicate the observed structural features

complete sterilization. This explains why some cultures were still contaminated (possibly due to endophytes or handling), even though 10 ppm AgNPs partially suppressed microbial growth. Statistically, ANOVA/DMRT results ($p<0.05$) showed significant differences between treatments regarding contamination; the treatment with the best regeneration (K2) recorded the lowest percentage of contamination. Further analysis also showed an inverse correlation between media contamination and regeneration results, confirming that AgNP application improved the overall culture performance (DMRT significance $\alpha=0.05$ in the data). Thus, the anticontaminant mechanisms of AgNPs (silver ions and ROS) were integrated into the culture medium, and statistical analysis confirmed the experimental findings that K2 significantly outperformed in all observed parameters.

In Conclusion, this study demonstrates that the interaction between culture medium composition and silver nanoparticle concentration significantly influences *in vitro* anther regeneration of tobacco. MS medium supplemented with 2.5 ppm silver nanoparticles produced the most favorable response, characterized by 100% callus formation, the highest shoot regeneration percentage, and successful rooting.

From a practical perspective, this optimized culture system provides an efficient and reproducible protocol for anther-derived plant regeneration and can be directly applied to doubled haploid production. The use of low-dose silver nanoparticles not only enhances regeneration efficiency but also reduces the risk of contamination, thereby improving the reliability of *in vitro* anther culture. Consequently, this protocol has strong potential to accelerate tobacco breeding programs by shortening the

breeding cycle, increasing the efficiency of homozygous line development, and supporting the rapid selection of superior genotypes for future variety improvement.

Acknowledgements

This research was funded by the University of Jember and conducted in the laboratory of Ecophysiology and Tissue Culture, Agronomy Study Program, Faculty of Agriculture, University of Jember. The explants used were from PT Tarutama Nusantara (TTN). The Scanning Electron Microscopy (SEM) analysis was carried out at the Laboratory of Pharmacognosy and Phytochemistry, Faculty of Pharmacy, University of Jember. The authors would also like to express their gratitude to the Institute for Research and Community Service (LP2M), University of Jember, for the support and facilitation provided throughout the research process.

References

Alejandro, S., Höller, S., Meier, B., Peiter, E., 2020. Manganese in plants: from acquisition to subcellular allocation. *Frontiers in Plant Science*. 11, 300. https://doi.org/10.3389/fpls.2020.00300

Alfarraj, N.S., Tarroum, M., Al-Qurainy, F., Nadeem, M., Khan, S., Salih, A.M., Shaikhaldein, H.O., Al-Hashimi, A., Alansi, S., Perveen, K., 2023. Biosynthesis of silver nanoparticles and exploring their potential of reducing the contamination of the *In Vitro* culture media and inducing the callus growth of *Rumex nervosus* explants. *Molecules*, 28, 3666. https://doi.org/10.3390/molecules28093666

Ali, A., Mohammad, S., Khan, M.A., Raja, N.I., Arif, M., Kamil, A., Mashwani, Z.-R., 2019. Silver nanoparticles elicited *In Vitro* callus cultures for accumulation of biomass and secondary metabolites in *Caralluma tuberculata*. *Artificial Cells, Nanomedicine, and Biotechnology*. 47, 715-724. https://doi.org/10.1080/21691401.2019.1577884

Ali., Nicolas, K.L.C., Akther, S., Torabi, A., Ebadi, A.A., Marfori-Nazarea, C.M., Mahender, A., 2021. Improved anther culture media for enhanced callus formation and plant regeneration in rice (*Oryza sativa* L.). *Plants*. 10, 839. https://doi.org/10.3390/plants10050839

Amaral, D.C., Brown, P. H., 2022. Foliar application of an inositol-based plant biostimulant boosts zinc accumulation in wheat grains: A μ-X-Ray fluorescence case study. *Frontiers in Plant Science*, 13. 837695. https://doi.org/10.3389/fpls.2022.837695

Ayala-Rodríguez, J.Á., Barrera-Ortiz, S., Ruiz-Herrera, L.F., López-Bucio, J., 2017. Folic acid orchestrates root development linking cell elongation with auxin response and acts independently of the target of rapamycin signaling in *Arabidopsis thaliana*. *Plant Science*, 264, 168-178. https://doi.org/10.1016/j.plantsci.2017.09.011

Azadi, M., Siavash Moghaddam, S., Rahimi, A., Pourakbar, L., Popović-Djordjević, J., 2021. Biosynthesized silver nanoparticles ameliorate yield, leaf photosynthetic pigments, and essential oil composition of garden thyme (*Thymus vulgaris* L.) Exposed to UV-B Stress. *Journal of Environmental Chemical Engineering*. 9, 105919. https://doi.org/10.1016/j.jece.2021.105919

[BPK RI] Badan Pemeriksa Keuangan Republik Indonesia., 2024. Laporan Keuangan Pemerintah Pusat Tahun 2023. https://www.bpk.go.id/assets/files/lkpp/2023/lkpp_2023_1717473846.pdf

[BPS] Badan Pusat Statistik., 2024. Produksi Tanaman Perkebunan (Ribu Ton) Tahun 2020 – 2023. https://www.bps.go.id/id/statistics-table/2/MTMyIzI=/produksi-tanaman-perkebunan.html.

Brdar-Jokanović, M., 2020. Boron toxicity and deficiency in agricultural plants. *International Journal of Molecular Sciences*. 21, 1424. https://doi.org/10.3390/ijms21041424

Cassells, A.C., 2012. Pathogen and biological contamination management in plant tissue culture: Phytopathogens, vitro pathogens, and vitro pests. *Methods Mol Biol.* 877, 57-80. https://doi.org/10.1007/978-1-61779-818-4_6

Che, P., Weaver, L.M., Wurtele, E.S., Nikolau, B.J., 2003. The role of biotin in regulating 3-Methylcrotonyl-Coenzyme a carboxylase expression in Arabidopsis. *Plant Physiology*. 131, 1479-1486. https://doi.org/10.1104/pp.013243

Chuprov–Netochin, R., Neskorodov, Y., Marusich, E., Mishutkina, Y., Volynchuk, P., Leonov, S., Skryabin, K., Ivashenko, A., Palme, K., Touraev, A., 2016. Novel small molecule modulators of plant growth and development identified by high-content screening with plant pollen. *BMC Plant Biology*. 16, 192. https://doi.org/10.1186/s12870-016-0875-4

Cosgrove, D.J., 2022. Building an extensible cell wall. *Plant Physiology.* 189, 1246-1277. https://doi.org/10.1093/plphys/kiac184

El-Fiki, A., El-Metabteb, G., Sayed, A.-H., Adly, M., 2015. Androgenesis induced in *Nicotiana alata* and the effect of gamma irradiation. *Notulae Scientia Biologicae*. 7, 66-71. https://doi.org/10.15835/nsb719477

Ewais, E.A., Elshazly, E.H., Ewais, E.A., Desouky, S.A., Elshazly, E.H., 2015. Evaluation of callus responses of *Solanum nigrum* L. exposed to biologically synthesized silver nanoparticles. *Nanoscience and Nanotechnology*. 5, 45-56. https://doi.org/10.5923/j.nn.20150503.01

Harris, K. D., Vanajah, T., Puvanitha, S., 2018. Effect of foliar application of boron and magnesium on growth and yield of green chilli (*Capsicum annum* & L.). *AGRIEAST: Journal of Agricultural Sciences*. 12, 26. https://doi.org/10.4038/agrieast.v12i1.49

Herawati, A., Yulaikah, S., 2011. Varietas unggul dan pemuliaan tembakau virginia di Indonesia. Balai Penelitian Tanaman Tembakau dan Serat. Repository Kementrian Pertanian. https://repository.pertanian.go.id/handle/123456789/15784

Hu, L., Zhou, K., Ren, G., Yang, S., Liu, Y., Zhang, Z., Li, Y., Gong, X., Ma, F., 2020. Myo-inositol mediates reactive oxygen species-induced programmed cell death via salicylic acid-dependent and ethylene-dependent pathways in apple. *Horticulture Research*. 7, 138. https://doi.org/10.1038/s41438-020-00357-2

Hu, X., Wei, X., Ling, J., Chen, J., 2021. Cobalt: an essential micronutrient for plant growth?. *Frontiers in Plant Science.* 12. 768523. https://doi.org/10.3389/fpls.2021.768523

Ikeuchi, M., Favero, D.S., Sakamoto, Y., Iwase, A., Coleman, D., Rymen, B., Sugimoto, K., 2019. Molecular mechanisms of plant regeneration. *Annual Review of Plant Biology*. 70, 377-406. https://doi.org/10.1146/annurev-arplant-050718-100434

Iori, V., Muzzini, V.G., Venditti, I., Casentini, B., Iannelli, M.A., 2023. Phytotoxic impact of bifunctionalized silver nanoparticles (AgNPs-Cit-L-Cys) and silver nitrate ($AgNO_3$) on chronically exposed callus cultures of *Populus nigra* L. *Environmental Science and Pollution Research*. 30, 116175-116185. https://doi.org/10.1007/s11356-023-30690-7

Khaldoun, K., Khizar, S., Saidi-Besbes, S., Zine, N., Errachid, A., Elaissari, A., 2025. Synthesis of silver nanoparticles as an antimicrobial mediator. *Journal of Umm Al-Qura University for Applied Sciences*. 11, 274-293. https://doi.org/10.1007/s43994-024-00159-5

Kimura, S., Vaattovaara, A., Ohshita, T., Yokoyama, K., Yoshida, K., Hui, A., Kaya, H., Ozawa, A., Kobayashi, M., Mori, I.C., Ogata, Y., Ishino, Y., Sugano, S.S., Nagano, M., Fukao, Y., 2023. Zinc deficiency-induced defensin-like proteins are involved in the inhibition of root growth in Arabidopsis. *The Plant Journal*. 115, 1071-1083. https://doi.org/10.1111/tpj.16281

Minibayeva, F., Beckett, R.P., Kranner, I., 2015. Roles of apoplastic peroxidases in plant response to wounding. *Phytochemistry*. 112, 122-129. https://doi.org/10.1016/j.phytochem.2014.06.008

More, P.R., Pandit, S., Filippis, A. De, Franci, G., Mijakovic, I., Galdiero, M., 2023. Silver nanoparticles: bactericidal and mechanistic approach against drug-resistant pathogens. *Microorganisms*. 11, 369. https://doi.org/10.3390/microorganisms11020369

Murthy, H.N., Lee, E.-J., Paek, K.-Y., 2014. Production of secondary metabolites from cell and organ cultures: strategies and approaches for biomass improvement and metabolite accumulation. *Plant Cell, Tissue and Organ Culture (PCTOC)*. 118, 1-16. https://doi.org/10.1007/s11240-014-0467-7

Ningrum, D.S., 2024. Pengaruh Konsentrasi Yeast Extract terhadap Pertumbuhan Kalus, Peningkatan Metabolit Sekunder (Flavonoid dan Fenolik) serta Aktivitas Antioksidan Kalus *Rubus fraxinifolius* secara *In Vitro* [Thesis]. Repository BKG, Malang: Universitas Brawijaya.

Nurhidayah, S., Purwoko, B.S., Dewi, I.S., Suwarno, W.B., Lubis, I., 2023. Agronomic performance and selection of green super rice doubled haploid lines from anther culture. *Biodiversitas Journal of Biological Diversity*. 24. https://doi.org/10.13057/biodiv/d240218

Rana, M.S., Bhantana, P., Sun, X., Imran, M., Shaaban, M., Moussa, M.G., Saleem, M.H., Elyamine, A.M., Binyamin, R., Alam, M., Afzal, J., Khan, I., Din, I.U., Ahmad, I., Younas, M., Kamran, M., Hu, C., 2020. Molybdenum as an essential element for crops: An overview. *Biomedical Journal of Scientific & Technical Research*. 24, 18535-18547. https://doi.org/10.26717/BJSTR.2020.24.004104

Rasud, Y., Bustaman, B., 2020. *In vitro* callus induction from clove (*Syzigium aromaticum* L.) leaves on medium containing various auxin concentrations. *Jurnal Ilmu Pertanian Indonesia.* 25, 67-72. https://doi.org/10.18343/jipi.25.1.67

Sari, N., Solmaz, I., 2021. Doubled haploid production in watermelon. *Methods Mol Biol.* 2289, 97-110. https://doi.org/10.1007/978-1-0716-1331-3_6

Satya, Hashmi, K., Gupta, S., Mishra, P., Khan, T., Joshi, S., 2024. The vital role of nanoparticles in enhancing plant growth and development. *Engineering proceedings*. 67, 48. https://doi.org/10.3390/engproc2024067048

Silvina, F., Isnaini, I., Ningsih, W., 2022. Induksi kalus daun binahong merah (*Basella rubra* L.) dengan pemberian 2,4-D dan kinetin. *Jurnal AGRO*. 8, 274-286. https://doi.org/10.15575/14273

Sood, S., Prasanna, P.S., Reddy, T.V., Gandra, S.V.S., 2021. Optimized protocol for development of androgenic haploids and doubled haploids in FCV tobacco (*Nicotiana tabacum*). *Methods Mol Biol.* 2288, 293-305. https://doi.org/10.1007/978-1-0716-1335-1_18

Statista., 2024. Gross Domestic Product (GDP) at Current Market Prices from Manufacture of Tobacco Products in Indonesia from 2014 to 2023. https://www.statista.com/statistics/1018748/indonesia-gdp-manufacture-of-tobacco-products/

Stoynova-Bakalova, E., Bakalov, D.V., Baskin, T.I., 2022. Ethylene represses the promoting influence of cytokinin on cell division and expansion of cotyledons in etiolated *Arabidopsis thaliana* seedlings. *PeerJ*. 10, e14315. https://doi.org/10.7717/peerj.14315

Sun, J., Wang, L., Li, S., Yin, L., Huang, J., Chen, C., 2017. Toxicity of silver nanoparticles to arabidopsis: Inhibition of root gravitropism by interfering with auxinpathway. *Environmental Toxicology and Chemistry*. 36, 2773-2780. https://doi.org/10.1002/etc.3833

Tefera, A.A., 2019. Review on application of plant tissue culture in plant breeding. *Journal of Natural Sciences Research*. 9, 20-25. https://doi.org/10.7176/JNSR

Wang, Q., Li, S., Li, J., Huang, D., 2024. The utilization and roles of nitrogen in plants. *Forests*. 15, 1191. https://doi.org/10.3390/f15071191

Wdowiak, A., Podgórska, A., Szal, B., 2024. Calcium in plants: an important element of cell physiology and structure, signaling, and stress responses. *Acta Physiologiae Plantarum*. 46, 108. https://doi.org/10.1007/s11738-024-03733-w

Xu, E., Liu, Y., Gu, D., Zhan, X., Li, J., Zhou, K., Zhang, P., Zou, Y., 2024. Molecular mechanisms of plant responses to copper: from deficiency to excess. *International Journal of Molecular Sciences*. 25, 6993. https://doi.org/10.3390/ijms25136993

Yan, A., Chen, Z., 2019. Impacts of silver nanoparticles on plants: A focus on the phytotoxicity and underlying mechanism. *International Journal of Molecular Sciences*. 20, 1003. https://doi.org/10.3390/ijms20051003

Yin, I.X., Jing, Z., Zhao, I.S., May, L.M., Li, Q., Chu, C.H., 2020. The antibacterial mechanism of silver nanoparticles and its application in dentistry. *International Journal of Nanomedicine*. 15, 2555-2562. https://doi.org/10.2147/IJN.S246764